

Bursty exposure on higher-order networks leads to nonlinear infection kernels

Guillaume St-Onge,^{1,2} Hanlin Sun,³ Antoine Allard,^{1,2} Laurent Hébert-Dufresne,^{1,4,5} and Ginestra Bianconi^{3,6}

¹*Département de physique, de génie physique et d'optique,
Université Laval, Québec (Québec), Canada G1V 0A6*

²*Centre interdisciplinaire en modélisation mathématique,
Université Laval, Québec (Québec), Canada G1V 0A6*

³*School of Mathematical Sciences, Queen Mary University of London, London, E1 4NS, United Kingdom*

⁴*Vermont Complex Systems Center, University of Vermont, Burlington, VT 05405*

⁵*Department of Computer Science, University of Vermont, Burlington, VT 05405*

⁶*The Alan Turing Institute, 96 Euston Rd, London NW1 2DB, United Kingdom*

The co-location of individuals in specific environments is an important prerequisite for exposure to infectious diseases on a social network. Standard epidemic models fail to capture the potential complexity of this scenario by (1) neglecting the hypergraph structure of contacts which typically occur through environments like workplaces, restaurants, and households; and by (2) assuming a linear relationship between the exposure to infected contacts and the risk of infection. Here, we leverage a hypergraph model to embrace the heterogeneity of different environments and the heterogeneity of individual participation in these environments. We find that a bursty exposure to environments can induce a nonlinear relationship between the number of infected participants and infection risk. This allows us to connect complex contagions based on nonlinear infection kernels and threshold models. We then demonstrate how conventional epidemic wisdom can break down with the emergence of discontinuous transitions, super-exponential spread, and regimes of hysteresis.

Mathematical models of epidemics play an increasingly important role in public health efforts and pandemic preparedness [1]. By providing insights about the interplay of the biological and sociological aspects of epidemics, models can test potential interventions in silico and suggest outcomes to expect [2]. However, large-scale forecasting comparisons show that statistical models often outperform mechanistic models that make assumptions about the details of disease spread [3].

In this letter, we look at the interplay of two commonly used assumptions in disease models: Random mixing and the linearity between infection risk and exposures to infected individuals. In almost all disease models, doubling the number of contacts between susceptible and infectious individuals doubles the risk of infection for the susceptible individuals. Some past work in mathematical biology has considered nonlinear infection rates [4, 5] but these models are rarely used in practice. Conversely, other fields such as sociology do often consider generalized contagion models, often dubbed complex contagions [6, 7]. In these complex contagions, having a nonlinear relationship between infection rate and sources of infection allows the model to consider mechanisms such as social reinforcement [8], where a set of multiple exposures can have more impact than the mere sum of unique exposures.

The mathematical convenience of assuming linearity when modeling infectious diseases comes at the price of two underlying assumptions. The first one implies that all contacts between susceptible and infectious individuals are effectively equivalent. This assumption has often been lifted using heterogeneous mathematical models where individuals are distinguished by some individual features such as their intrinsic susceptibility or reaction to the infection [9, 10], relaxing the mass-action assumption directly [11, 12], or by specifying an underlying contact network [13, 14]. There is however mounting evidence that social interactions go beyond pairwise interactions and require a higher-order representation [15].

The second underlying assumption says that all increments in the total exposure to infectious individuals (measured for example as a viral inoculum) are equivalent. Evidence associated with the minimal infective dose of different infectious diseases shows that not all exposures are equal, and that some minimal dose might be required for an infection to likely occur. More precisely, the ID₅₀ value is a measure of the dose needed to cause an infection in 50% of individuals. These concepts are needed because our immune system is usually able to handle microscopic challenges from viruses and bacteria alike. While an infective dose of tuberculosis might only require between 1 and 5 bacteria [16], other diseases such as some enterics might require up to 10⁹ pathogenic particles [17], and others like common respiratory infections still require further study [18]. Accounting for minimal infectious doses could require the need for nonlinear infection rates [19].

To study the effect of simultaneously relaxing these two assumptions, we consider a social structure where individuals attend a certain number of environments such as work places, gyms, or supermarkets. This division of contact structure in environments is motivated by the known role of superspreading events, which are for example critical to the ongoing spread of COVID-19 [20, 21]. Both the temporal patterns and group structures of these events will undoubtedly affect epidemics where a certain level of exposure within a certain time window is needed to confidently spark an infection. Interestingly, available case data highlight how there is no expected size or duration for such events. Transmission is highly context dependent on the settings (e.g., ventilation) and activity (e.g., singing or shouting) such that the resulting superspreading events are heterogeneous in size, duration and attack rate, as shown in Fig. 1.

Mathematically, we represent the contact structure as a hypergraph where each environment γ is described by a hyperedge connecting m_γ nodes (individuals) and where each node

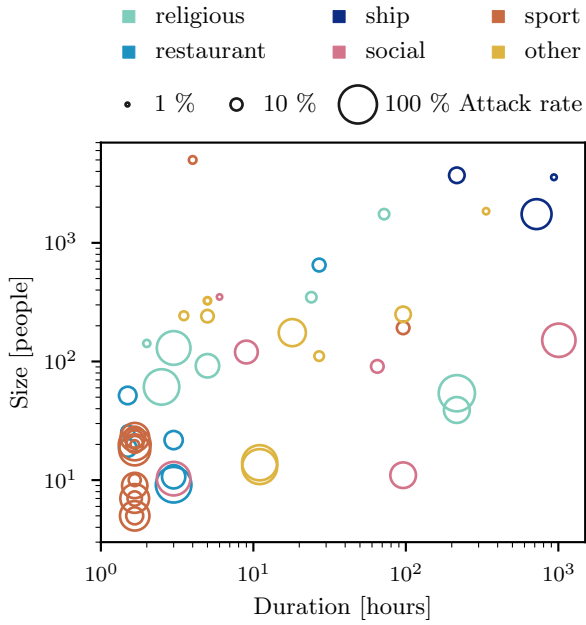


FIG. 1. Scatter plot of superspreading events of COVID-19 where the number of people involved (size), the duration of the event, and the resulting proportion of infected individuals (attack rate) are all available. Other than the intuitive result that larger events (weddings, cruises) tend to last longer than smaller events (meals), there is no clear relationship in the data. Both the size and duration of important events are highly heterogeneous and poorly correlated with the attack rate of the event, hinting at heterogeneous transmission rates based on the local context and environmental conditions.

r is incident to k_r hyperedges. We then study the role of the underlying spatiotemporal patterns of co-location of individuals in the population.

Nonlinear infection kernels from bursty exposure. We denote $P(\tau)$ the distribution of participation time τ of an individual to a given environment. During the exposure period, we assume that the considered individual has κ interactions with infectious individuals affiliated to the same hyperedge, and receive an infective dose from these interactions. These are taken to be random encounters, so κ is drawn from a Poisson distribution $\pi(\kappa) = z^\kappa e^{-z}/\kappa!$ with expectation $z = \beta f(m)\tau\rho$, where ρ is the probability that a random individual belonging to the hyperedge is infected, m is the total number of individuals belonging to the hyperedge γ and β is a scaling parameter. The function $f(m)$ can model different physical scenarios. If $f(m) \propto m$, the expected number of interactions with infectious individuals z scales linearly with the hyperedge size. On the contrary, if $f(m) = \text{cst.}$, the number of infectious individuals met in a given environment is independent of m . Most realistic scenarios should fall in between these two.

We also consider different minimal infective doses. In the simplest case, a single interaction is sufficient to become infected. Hence the probability of infection for a susceptible individual, exposed for a duration τ to an environment where a fraction ρ of the $m-1$ other individuals are infected, is given

by

$$T_{\tau,m}(\rho) = 1 - e^{-\tau/\tau_c}, \quad (1)$$

where $\tau_c \equiv [f(m)\beta\rho]^{-1}$ sets the characteristic time scale to have an interaction with an infected individual.

More generally, we can consider that an individual is infected if it receives a dose from K encounters. This can be understood in terms of a higher ID_{50} value of the disease for instance. We can express the probability of infection $T_{\tau,m}(\rho)$ as

$$T_{\tau,m}(\rho) = 1 - \sum_{\kappa=0}^{K-1} \frac{1}{\kappa!} \left(\frac{\tau}{\tau_c}\right)^\kappa e^{-\tau/\tau_c}. \quad (2)$$

This perspective is analogous to standard *threshold* models [22–24], where K would be the threshold value to become infected. We will limit the discussion to the cases $K = 1$ and $K = 2$, but the following arguments are easily generalizable to arbitrary K .

We now consider different probability distributions $P(\tau)$ for the participation time τ of an individual to a given environment. We want to evaluate the probability $\theta_m = \theta_m(\rho)$ that an individual is infected due to its exposure to a hyperedge γ of size $m_\gamma = m$, where the $m-1$ other individuals are infected with probability ρ . It is given by

$$\theta_m(\rho) = \int_1^{\mathcal{T}} d\tau P(\tau) T_{\tau,m}(\rho). \quad (3)$$

If the participation time is constant, i.e., $P(\tau) = \delta(\tau - \tau')$, we obtain in the limit $\rho \ll 1$ that the probability of infection is $\theta_m(\rho) \propto \rho^\nu$ with $\nu = K$. Therefore, if a single interaction is sufficient for the transmission, we recover that the probability of infection is linear in the fraction of infected individuals ρ attending the same environment, and only for $K > 1$ we can consider supra-linear ($\nu > 1$) dependence on ρ , with $\nu \in \mathbb{N}$. This scaling remains unchanged for $K \in \{1, 2\}$ if $P(\tau)$ has a well-defined mean and variance.

However, the scenario changes if we consider a bursty exposure [25–31]. Let us consider a distribution $P(\tau) = C_\alpha \tau^{-\alpha-1}$ for the participation time, with C_α a normalization constant, $\alpha > 0$ and $\tau \in [1, \mathcal{T}]$, which induces bursty interaction patterns (see supplementary material). With a threshold $K = 1$, the probability θ_m corresponds to

$$\theta_m(\rho) = 1 - C_\alpha \text{Ei}_{\alpha+1}(1/\tau_c) + C_\alpha \mathcal{T}^{-\alpha} \text{Ei}_{\alpha+1}(\mathcal{T}/\tau_c). \quad (4)$$

In the limit $\mathcal{T}/\tau_c \gg 1$, and as long as $1/\tau_c \ll 1$, we can expand this formula, obtaining the scaling $\theta_m \propto \tau_c^{-\nu} \propto \rho^\nu$, where

$$\nu = \begin{cases} \alpha & \text{for } \alpha \in (0, 1), \\ 1 & \text{for } \alpha \geq 1. \end{cases} \quad (5)$$

For $\rho \ll 1$, this implies that θ_m is larger for broader distributions $P(\tau)$. Note that the regime of validity of this expansion is interpreted as follows: the minimal participation time

is typically insufficient to interact with an infected individual ($1 \ll \tau_c$), but the maximal participation time is ($\mathcal{T} \gg \tau_c$).

If we consider $K > 1$, we can obtain real exponents $\nu > 1$. For instance, assuming $K = 2$, then $\theta_m(\rho)$ is defined as

$$\theta_m(\rho) = \int_1^{\mathcal{T}} d\tau P(\tau) \left[1 - \left(1 + \frac{\tau}{\tau_c} \right) e^{-\tau/\tau_c} \right]. \quad (6)$$

Taking again $P(\tau) = C_\alpha \tau^{-\alpha-1}$, in the limit $\mathcal{T}/\tau_c \gg 1$ and $1/\tau_c \ll 1$, we obtain

$$\nu = \begin{cases} \alpha & \text{for } \alpha \in (0, 2) \\ 2 & \text{for } \alpha \geq 2. \end{cases} \quad (7)$$

This is validated in Fig. 2(a) for different values of α .

More generally, the combination of bursty exposure and an arbitrary minimal number of infective doses K leads to a nonlinear infection kernel $\theta_m(\rho) \propto \rho^\nu$, with $\nu \in \mathbb{R}^+$. From now on, we ignore the underlying threshold K and focus on the resulting effective model parametrized by ν .

Epidemic spreading with nonlinear infection kernel. To illustrate the consequences of a nonlinear infection kernel, we now consider spreading dynamics taking place on a hypergraph. To simplify the model, we assume that the distribution $P(\tau)$ of participation time is independent of the environment. Furthermore, we assume that the average total participation time of a single individual to all of its environments is much smaller than the duration of the considered temporal window, i.e., $k_{\max} \langle \tau \rangle \ll \mathcal{T}$ around nodes of maximal degree k_{\max} . This way, we can consider the participation time of an individual to different environments as independent random variables.

For simplicity, we consider a Susceptible-Infectious-Susceptible model. By considering an ensemble of hypergraphs with distribution $\tilde{P}(k)$ for the degree of the nodes and distribution $\hat{P}(m)$ for the size of the hyperedges, we can study the contagion process on an annealed structure in the thermodynamic limit. At each time slice $t = 1, 2, \dots$, we assume that stubs of all nodes are matched uniformly at random with the hyperedges. An infected node becomes susceptible with probability μ , while a susceptible node gets infected through an hyperedge γ with probability θ_γ . Under those assumptions, the marginal probability for node r to be infected only depends on its degree, $\rho_r \mapsto \rho_{k_r}$, and the probability θ_γ only depends on the size of the hyperedge, $\theta_\gamma \mapsto \theta_{m_\gamma}$. The global prevalence is then simply $I = \sum_k \rho_k \tilde{P}(k)$.

The evolution of the system is described by

$$\rho_k(t+1) = (1-\mu)\rho_k(t) + (1-\rho_k(t))\Theta_k, \quad (8)$$

where $\Theta_k(\bar{\rho}) = 1 - [1 - \bar{\theta}(\bar{\rho})]^k$ is the average probability for a susceptible node of degree k to get infected. $\bar{\rho}(t)$ is the average probability that a node belonging in any hyperedge is infected and $\bar{\theta}(\bar{\rho})$ is the average probability for a susceptible node to get infected in any hyperedge,

$$\bar{\rho}(t) = \sum_k \rho_k(t) \frac{k\tilde{P}(k)}{\langle k \rangle} \quad \text{and} \quad \bar{\theta}(\bar{\rho}) = \sum_m \bar{\theta}_m(\bar{\rho}) \frac{m\hat{P}(m)}{\langle m \rangle}, \quad (9)$$

where $\bar{\theta}_m(\bar{\rho})$ is the average probability for a node to get infected in an hyperedge of size m . Because of the annealed structure, $\bar{\theta}_m(\bar{\rho})$ is just the average of θ_m over a binomial distribution, i.e.,

$$\bar{\theta}_m(\bar{\rho}) = \sum_{i=0}^{m-1} \binom{m-1}{i} \bar{\rho}^i (1-\bar{\rho})^{m-1-i} \theta_m\left(\frac{i}{m-1}\right), \quad (10)$$

with $\theta_m(\rho)$ defined at Eq. (3).

Figure 2(b) shows a first consequence of the nonlinear kernel: the apparition of supra-exponential growth for the global prevalence $I(t)$ when $\nu > 1$. For $\nu \leq 1$, we instead have a standard exponential growth.

In the steady state of the epidemic dynamics defined in Eq. (8), we obtain a self-consistent solution

$$\rho_k^* = \frac{\Theta_k^*}{\mu + \Theta_k^*} \quad \text{and} \quad \bar{\rho}^* = \sum_k \tilde{P}(k) \frac{k}{\langle k \rangle} \frac{\Theta_k^*}{\mu + \Theta_k^*} \equiv G(\bar{\rho}^*), \quad (11)$$

since Θ_k is a function of $\bar{\rho}$.

For contagions with a nonlinear infection kernel, the phase transition associated with the order parameter I^* can be continuous or discontinuous with a bistable regime. Hence, we define the *invasion* threshold β_c as the limit value such that for all $\beta > \beta_c$, the absorbing state $I^* = 0$ is unstable. We also define the *persistence* threshold β_p as the limit value such that for all $\beta < \beta_p$, the absorbing state $I^* = 0$ is globally attractive. For continuous phase transitions, β_c and β_p coincide, and is called the epidemic threshold; for a discontinuous phase transition with a bistable regime, $\beta_p < \beta_c$, and for all $\beta \in (\beta_p, \beta_c)$, there are typically three solutions, $I_1^* = 0$ and $I_2^*, I_3^* > 0$, with I_1^* and I_3^* locally stable.

The invasion threshold β_c can be found by imposing $G'(0) = 1$, the persistence threshold β_p of the discontinuous transition can be obtained by imposing both $\bar{\rho}^* = G(\bar{\rho}^*)$ and $G'(\bar{\rho}^*) = 1$, and any tricritical point can be found by imposing $G'(0) = 1$ and $G''(0) = 0$.

In the supplementary material, we obtain an exact self-consistent expression for the invasion threshold, and using again an asymptotic development, we find

$$\beta_c \propto \left(\frac{\mu \langle m \rangle \langle k \rangle}{\langle m(m-1) \rangle^{1-\nu} [f(m)]^\nu \langle k^2 \rangle} \right)^{1/\nu}. \quad (12)$$

As illustrated in Fig. 2(c), the invasion threshold can become very small for $\nu < 1$ (vanishing for $\nu \rightarrow 0$), even for homogeneous $\tilde{P}(k)$ and $\hat{P}(m)$. We have $\beta_c \approx 10^{-5}$ for $\nu = 0.5$, with Poisson distributions of mean $\langle m \rangle = 10$ and $\langle k \rangle = 5$. Increasing the value of ν leads to a larger invasion threshold, assuming $f(m)$ has a reasonable form. This is consistent with the fact that the mean exposure time $\langle \tau \rangle$ is larger for smaller ν ; surprisingly, the invasion threshold is small but non-vanishing for $0 < \nu < 1$, even though $\langle \tau \rangle$ diverges in the limit $\mathcal{T} \rightarrow \infty$.

Supra-linear kernel allows for a discontinuous phase transition [Fig. 2(c)]. The minimal value ν_c for which it is possible is given by a tricritical point. In the supplementary material,

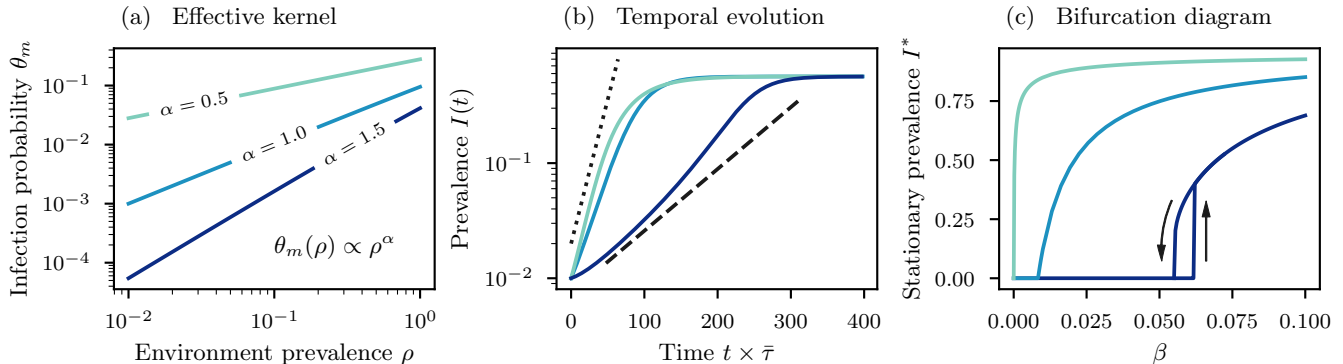


FIG. 2. Properties of contagions with nonlinear infection kernels induced by bursty exposure. We use a threshold ($K = 2$) with a power-law distribution of participation time $P(\tau) \propto \tau^{-\alpha-1}$, a time window $\mathcal{T} \rightarrow \infty$, and $f(m) = 1$. (a) Effective infection kernel using $\beta = 0.1$. For $\tau_c^{-1} \ll 1$, the infection probability has a power-law scaling $\theta_m(\rho) \propto \rho^\nu$ with $\nu = \alpha$ if $K \geq \alpha$. (b)-(c) We use a Poisson distributions for both $\hat{P}(k)$ and $\hat{P}(m)$, with $\langle k \rangle = 5$ and $\langle m \rangle = 10$, and set $\mu = 0.05$. We use the annealed system [Eqs. (8-10)]. (b) Supra-linear kernel $\nu > 1$ leads to a supra-exponential growth for the global prevalence $I(t)$. We use $\beta = 5 \times 10^{-4}$, $\beta = 0.025$ and $\beta = 0.077$ for $\nu = 0.5$, $\nu = 1$ and $\nu = 1.5$ respectively. $\bar{\tau}$ is the median participation time associated with $P(\tau)$. (c) The bifurcation diagram in the stationary state ($t \rightarrow \infty$) can be continuous or discontinuous with a bistable regime. Sub-linear and linear kernels $\nu \leq 1$ lead to a continuous phase transition, and the invasion threshold β_c vanishes for $\nu \rightarrow 0$. Supra-linear kernel $\nu > 1$ can lead to a discontinuous phase transition with a bistable regime.

we provide a self-consistent expression to solve for tricritical points. Although exact solutions require numerical evaluation, we get three insights from an asymptotic expansion. (i) $\nu > 1$ is necessary in order to have a discontinuous phase transition, but it is not sufficient: ν_c depends on the first three moments of $\hat{P}(k)$, and in a more complicated manner on the distribution $\hat{P}(m)$. (ii) It is necessary to have $\hat{P}(m) > 0$ for at least one value $m > 2$, i.e., environments of size $m = 2$ cannot lead to a discontinuous phase transition. (iii) A more heterogeneous $\hat{P}(k)$ leads to a larger ν_c . Similar observations were made in Ref. [32] for hyperedges of size $m \leq 3$.

Conclusion. Our framework captures many properties usually overlooked for the sake of simplicity in epidemic models: the higher-order structure and temporal heterogeneity of human activity, thresholding effects over multiple exposures due to the host immune system, as well as differences in individual susceptibility or local transmission in different environments—in the supplementary material, we show that our results are robust to these other sources of heterogeneity. In particular, we show that combining thresholding effects, temporal heterogeneity and correlations in space due to the higher-order structure of social networks leads to nonlinear infection kernels. This formally provides a connection between complex contagions based on nonlinear infection kernels [33] and threshold models [22–24].

On a theoretical, this work allows for a deeper understanding of how burstiness affects epidemic spreading. Previous works [34] have shown that bursty interactions can slow down the spreading for simple contagions on temporal networks, while burstiness can both accelerate or decelerate the spreading in threshold models [35, 36]. Here we find that bursty exposure to the hyperedges of a hypergraph can significantly speed up the epidemic spreading and minimize the invasion threshold β_c . It is worth mentioning that our results

hinge on the fact that we considered a fixed minimal participation time $\tau_{\min} = 1$. In the supplementary material, we show that if instead we fix the average participation time $\langle \tau \rangle$, there exists an optimal temporal heterogeneity α^* that minimizes the invasion threshold β_c , and maximizes early spread.

On the epidemiological level, our results challenge a key assumption of most epidemic models and ask: Why assume a linear relationship between the number of infectious contacts and infection risk? This question is critical since three of the basic insights gathered from epidemic models break down under nonlinear infection kernels. First, they can lead to a non-monotonic (or discontinuous) relationship between disease transmission and the resulting epidemic size. Second, they can lead to faster than exponential spreading, contrary to one of our most common assumptions about disease. Finally, they can lead to bistable regimes where the same epidemic in the same population could lead to either a macroscopic outbreak or a disease-free state depending only on initial conditions.

The mathematical framework we used to describe epidemic spreading on hypergraphs shares many properties with existing approaches [32, 37–39], while allowing more flexibility for the heterogeneity of hyperedges. One shared aspect is the mean-field or annealed assumption, which suppresses *dynamical correlations*—if an environment at time t contains i infected nodes, at time $t + 1$ the number of infected nodes is distributed according to a binomial, irrespective of the value of i . This is a reasonable assumption for certain environments, such as a supermarket, but less so for an office. Future works could investigate the interplay between dynamical correlations, nonlinear kernels, and spatiotemporal heterogeneity, using for instance approximate master equations [40–43].

Altogether, our conclusions stress the need to embrace heterogeneity in disease modeling; in the infection dynamics it-

self, in patterns of temporal activity, and in the higher-order structure of contact networks. Epidemics should be seen as the result of a collective process, where higher-order structure and temporal patterns can drive complex dynamics.

This work was supported by the Fonds de recherche du Québec – Nature et technologies (G.S.), the Natural Sciences and Engineering Research Council of Canada (G.S., A.A.), the Sentinelle Nord program from the Canada First Research Excellence Fund (G.S., A.A.), the National Institutes of Health 1P20 GM125498-01 Centers of Biomedical Research Excellence Award (L.H.-D.), the Royal Society (IEC\NSFC\191147; G.B.), and by the Chinese Scholarship Council (H.S.).

-
- [1] C. Rivers, J.-P. Chretien, S. Riley, J. A. Pavlin, A. Woodward, D. Brett-Major, I. Maljkovic Berry, L. Morton, R. G. Jarman, M. Biggerstaff, M. A. Johansson, N. G. Reich, D. Meyer, M. R. Snyder, and S. Pollett, Using “outbreak science” to strengthen the use of models during epidemics, *Nat. Commun.* **10**, 3102 (2019).
- [2] J. M. Epstein, Why Model?, *JASSS* **11**, 12 (2008).
- [3] M. Biggerstaff, M. Johansson, D. Alper, L. C. Brooks, P. Chakraborty, D. C. Farrow, S. Hyun, S. Kandula, C. McGowan, N. Ramakrishnan, R. Rosenfeld, J. Shaman, R. Tibshirani, R. J. Tibshirani, A. Vespignani, W. Yang, Q. Zhang, and C. Reed, Results from the second year of a collaborative effort to forecast influenza seasons in the United States, *Epidemics* **24**, 26 (2018).
- [4] W.-m. Liu, S. A. Levin, and Y. Iwasa, Influence of nonlinear incidence rates upon the behavior of SIRS epidemiological models, *J. Math. Biol.* **23**, 187 (1986).
- [5] H. W. Hethcote and P. van den Driessche, Some epidemiological models with nonlinear incidence, *J. Math. Biol.* **29**, 271 (1991).
- [6] D. Centola, *How Behavior Spreads: The Science of Complex Contagions* (Princeton University Press, 2018).
- [7] S. Lehmann and Y.-. Ahn, *Complex Spreading Phenomena in Social Systems* (Springer, 2018).
- [8] D. Centola, The Spread of Behavior in an Online Social Network Experiment, *Science* **329**, 1194 (2010).
- [9] S. N. Busenberg, M. Iannelli, and H. R. Thieme, Global Behavior of an Age-Structured Epidemic Model, *SIAM J. Math. Anal.* **22**, 1065 (1991).
- [10] Z. Feng and H. R. Thieme, Endemic Models with Arbitrarily Distributed Periods of Infection I: Fundamental Properties of the Model, *SIAM J. Appl. Math.* **61**, 803 (2000).
- [11] H. W. Hethcote and J. W. Van Ark, Epidemiological models for heterogeneous populations: Proportionate mixing, parameter estimation, and immunization programs, *Math. Biosci.* **84**, 85 (1987).
- [12] H. W. Hethcote, Modeling heterogeneous mixing in infectious disease dynamics, in *Models for Infectious Human Diseases: Their Structure and Relation to Data* (Cambridge University Press, 1996) 1st ed., pp. 215–238.
- [13] R. Pastor-Satorras and A. Vespignani, Epidemic Spreading in Scale-Free Networks, *Phys. Rev. Lett.* **86**, 3200 (2001).
- [14] R. Pastor-Satorras, C. Castellano, P. Van Mieghem, and A. Vespignani, Epidemic processes in complex networks, *Rev. Mod. Phys.* **87**, 925 (2015).
- [15] F. Battiston, G. Cencetti, I. Iacopini, V. Latora, M. Lucas, A. Patania, J.-G. Young, and G. Petri, Networks beyond pairwise interactions: Structure and dynamics, *Phys. Rep.* **874**, 1 (2020).
- [16] V. Balasubramanian, E. H. Wiegand, B. T. Taylor, and D. W. Smith, Pathogenesis of tuberculosis: Pathway to apical localization, *Tuber. Lung Dis.* **75**, 168 (1994).
- [17] R. C. LaRocque and S. B. Calderwood, Syndromes of enteric infection, in *Mandell, Douglas, and Bennett’s Principles and Practice of Infectious Diseases* (Elsevier, 2015) pp. 1238–1247.
- [18] T. P. Weber and N. I. Stilianakis, Inactivation of influenza A viruses in the environment and modes of transmission: A critical review, *J. Infect.* **57**, 361 (2008).
- [19] J. Anttila, L. Mikonranta, T. Ketola, V. Kaitala, J. Laakso, and L. Ruokolainen, A mechanistic underpinning for sigmoid dose-dependent infection, *Oikos* **126**, 910 (2017).
- [20] F. Wong and J. J. Collins, Evidence that coronavirus super-spreading is fat-tailed, *Proc. Natl. Acad. Sci. U.S.A.* **117**, 29416 (2020).
- [21] B. M. Althouse, E. A. Wenger, J. C. Miller, S. V. Scarpino, A. Allard, L. Hébert-Dufresne, and H. Hu, Superspreading events in the transmission dynamics of SARS-CoV-2: Opportunities for interventions and control, *PLOS Biol.* **18**, e3000897 (2020).
- [22] M. Granovetter, Threshold Models of Collective Behavior, *Am. J. Sociol.* **83**, 1420 (1978).
- [23] D. J. Watts, A simple model of global cascades on random networks, *Proc. Natl. Acad. Sci. U.S.A.* **99**, 5766 (2002).
- [24] P. S. Dodds and D. J. Watts, Universal Behavior in a Generalized Model of Contagion, *Phys. Rev. Lett.* **92**, 218701 (2004).
- [25] M. Karsai, H.-H. Jo, and K. Kaski, *Bursty Human Dynamics* (Springer International Publishing, 2018).
- [26] M. Karsai, K. Kaski, A.-L. Barabási, and J. Kertész, Universal features of correlated bursty behaviour, *Sci. Rep.* **2**, 397 (2012).
- [27] P. Holme and J. Saramäki, Temporal networks, *Phys. Rep.* **519**, 97 (2012).
- [28] C. Cattuto, W. Van den Broeck, A. Barrat, V. Colizza, J.-F. Pinton, and A. Vespignani, Dynamics of Person-to-Person Interactions from Distributed RFID Sensor Networks, *PLOS ONE* **5**, e11596 (2010).
- [29] J. Stehlé, A. Barrat, and G. Bianconi, Dynamical and bursty interactions in social networks, *Phys. Rev. E* **81**, 035101 (2010).
- [30] K. Zhao, J. Stehlé, G. Bianconi, and A. Barrat, Social network dynamics of face-to-face interactions, *Phys. Rev. E* **83**, 056109 (2011).
- [31] G. Cencetti, F. Battiston, B. Lepri, and M. Karsai, Temporal properties of higher-order interactions in social networks, *arXiv* , 2010.03404 (2020).
- [32] N. W. Landry and J. G. Restrepo, The effect of heterogeneity on hypergraph contagion models, *Chaos* **30**, 103117 (2020).
- [33] W.-m. Liu, H. W. Hethcote, and S. A. Levin, Dynamical behavior of epidemiological models with nonlinear incidence rates, *J. Math. Biol.* **25**, 359 (1987).
- [34] M. Karsai, M. Kivelä, R. K. Pan, K. Kaski, J. Kertész, A.-L. Barabási, and J. Saramäki, Small but slow world: How network topology and burstiness slow down spreading, *Phys. Rev. E* **83**, 025102 (2011).
- [35] F. Karimi and P. Holme, Threshold model of cascades in empirical temporal networks, *Physica A* **392**, 3476 (2013).
- [36] S. Unicomb, G. Iñiguez, J. P. Gleeson, and M. Karsai, Dynamics of cascades on burstiness-controlled temporal networks, *Nat. Commun.* **12**, 133 (2021).
- [37] I. Iacopini, G. Petri, A. Barrat, and V. Latora, Simplicial models of social contagion, *Nat. Commun.* **10**, 1 (2019).

- [38] B. Jhun, M. Jo, and B. Kahng, Simplicial SIS model in scale-free uniform hypergraph, *J. Stat. Mech.* **2019**, 123207 (2019).
- [39] G. Ferraz de Arruda, G. Petri, and Y. Moreno, Social contagion models on hypergraphs, *Phys. Rev. Research* **2**, 023032 (2020).
- [40] L. Hébert-Dufresne, P.-A. Noël, V. Marceau, A. Allard, and L. J. Dubé, Propagation dynamics on networks featuring complex topologies, *Phys. Rev. E* **82**, 036115 (2010).
- [41] D. J. P. O'Sullivan, G. J. O'Keeffe, P. G. Fennell, and J. P. Gleeson, Mathematical modeling of complex contagion on clustered networks, *Front. Phys.* **3**, 71 (2015).
- [42] G. St-Onge, V. Thibeault, A. Allard, L. J. Dubé, and L. Hébert-Dufresne, Master equation analysis of mesoscopic localization in contagion dynamics on higher-order networks, [arXiv:2004.10203](https://arxiv.org/abs/2004.10203) (2020).
- [43] G. St-Onge, V. Thibeault, A. Allard, L. J. Dubé, and L. Hébert-Dufresne, Social confinement and mesoscopic localization of epidemics on networks, [arXiv:2003.05924](https://arxiv.org/abs/2003.05924) (2020).
- [44] S. Nadarajah, Exact distribution of the product of m gamma and n Pareto random variables, *J. Comput. Appl. Math.* **235**, 4496 (2011).

Bursty exposure on higher-order networks leads to nonlinear infection kernels

— Supplementary Material —

Guillaume St-Onge,^{1,2} Hanlin Sun,³ Antoine Allard,^{1,2} Laurent Hébert-Dufresne,^{1,4,5} and Ginestra Bianconi^{3,6}

¹*Département de physique, de génie physique et d'optique,
Université Laval, Québec (Québec), Canada G1V 0A6*

²*Centre interdisciplinaire en modélisation mathématique,
Université Laval, Québec (Québec), Canada G1V 0A6*

³*School of Mathematical Sciences, Queen Mary University of London, London, E1 4NS, United Kingdom*

⁴*Vermont Complex Systems Center, University of Vermont, Burlington, VT 05405*

⁵*Department of Computer Science, University of Vermont, Burlington, VT 05405*

⁶*The Alan Turing Institute, 96 Euston Rd, London NW1 2DB, United Kingdom*

POWER-LAW DISTRIBUTION OF PARTICIPATION TIME LEADS TO BURSTY INTERACTIONS

Correlations and memory effects are often responsible for the emergence of a bursty temporal sequence of events or interactions [1]. To study the impact of burstiness, renewal processes with general inter-event time distributions are often used to model the departure from a standard Poisson process, where the inter-event time is exponentially distributed, and the number of events n in any time window is Poisson distributed.

In our model, we are interested in the number of interactions happening in a particular environment, in a time window \mathcal{T} . This number is correlated with the participation time τ of the individual to the environment. For a given τ , n is Poisson distributed by definition,

$$p(n|\tau) = \frac{\omega^n e^{-\omega}}{n!},$$

where $\omega \equiv \beta f(m)\tau$. Note that n and $p(n|\tau)$ are related to κ and $\pi(\kappa)$ in the main text— κ are the interactions with infected individuals.

When the participation time is homogeneous, e.g., $P(\tau) = \delta(\tau - \tau')$, the number of interactions in a time window of size \mathcal{T} ,

$$p(n) = \int_1^{\mathcal{T}} p(n|\tau)P(\tau)d\tau,$$

is also Poisson distributed. However, as soon as $P(\tau)$ departs from a sharply peaked probability density function, $p(n)$ moves away from a Poisson distribution as well. In the case of a power-law distribution $P(\tau) = C_\alpha \tau^{-\alpha-1}$, it can be shown using Laplace method that

$$p(n) \propto n^{-\alpha-1},$$

for large n and $\beta f(m) < n - \alpha - 1 < \beta f(m)\mathcal{T}$. This important departure from a Poisson distribution is a signature of a bursty dynamics.

ALTERNATE FORM FOR $\bar{\theta}_m(\bar{\rho})$

For the evolution of the annealed SIS model, it is more efficient to rewrite $\bar{\theta}_m(\bar{\rho})$ using the properties of the binomial distribution. Combining Eqs. (2), (3) and (10) in the main text, we obtain

$$\bar{\theta}_m(\bar{\rho}) = 1 - \lim_{\lambda \rightarrow 1} \sum_{\kappa=0}^{K-1} \frac{1}{\kappa!} \frac{d^\kappa}{d\lambda^\kappa} \int_1^{\mathcal{T}} (1 - \bar{\rho} + \bar{\rho}e^{-\lambda\eta_m\tau})^{m-1} P(\tau)d\tau,$$

for a general threshold K and where $\eta_m \equiv \beta f(m)/(m-1)$.

CHARACTERIZATION OF THE PHASE TRANSITION

As discussed in the main text, the phase transition is characterized by $G(\bar{\rho}^*)$. In this section, we derive self-consistent equations for both the invasion threshold β_c and any tricritical point (β_c, ν_c) , where $\nu_c \equiv \alpha_c - 1$ is a limit value for the nonlinear kernel exponent separating a continuous and a discontinuous phase transition.

All time-varying quantities are assumed to have reached the steady state—to simplify the notation, we drop the asterisk. First, let us rewrite $G(\bar{\rho})$ [Eq. (11) in the main text] and its derivatives as

$$\begin{aligned} G(\bar{\rho}) &= \frac{1}{\langle k \rangle} \left\langle \frac{k\Theta_k}{\mu + \Theta_k} \right\rangle, \\ G'(\bar{\rho}) &= \frac{1}{\langle k \rangle} \left\langle \frac{k\Theta'_k(\bar{\rho})}{\mu + \Theta_k} - \frac{k\Theta_k\Theta'_k(\bar{\rho})}{(\mu + \Theta_k)^2} \right\rangle, \\ G''(\bar{\rho}) &= \frac{1}{\langle k \rangle} \left\langle \frac{k\Theta''_k(\bar{\rho})}{\mu + \Theta_k} - \frac{2k[\Theta'_k(\bar{\rho})]^2}{(\mu + \Theta_k)^2} - \frac{k\Theta_k\Theta''_k(\bar{\rho})}{(\mu + \Theta_k)^2} + \frac{2k\Theta_k[\Theta'_k(\bar{\rho})]^2}{(\mu + \Theta_k)^3} \right\rangle. \end{aligned}$$

In the limit $\bar{\rho} \rightarrow 0$, we have $\bar{\theta} \rightarrow 0$, which implies $\Theta_k \rightarrow 0$ for all k and

$$\begin{aligned} \Theta'_k(0) &= k\bar{\theta}'(0), \\ \Theta''_k(0) &= k\bar{\theta}''(0) - k(k-1)[\bar{\theta}'(0)]^2. \end{aligned}$$

Therefore, we have

$$G'(0) = \frac{\langle k \rangle}{\mu} \bar{\theta}'(0), \quad (\text{S1a})$$

$$G''(0) = \frac{1}{\mu} \left\{ \langle k^2 \rangle \bar{\theta}''(0) - \left(\langle k^2(k-1) \rangle + \frac{2\langle k^3 \rangle}{\mu} \right) [\bar{\theta}'(0)]^2 \right\}. \quad (\text{S1b})$$

Second, $\bar{\theta}(\bar{\rho})$ is rewritten as

$$\bar{\theta}(\bar{\rho}) = \frac{1}{\langle m \rangle} \langle m\bar{\theta}_m(\bar{\rho}) \rangle, \quad (\text{S2})$$

hence it depends on $\bar{\rho}$ only through $\bar{\theta}_m(\bar{\rho})$.

Finally, it is straightforward to obtain the derivatives of Eq. (10) in the main text for $\bar{\rho} = 0$, i.e.,

$$\bar{\theta}'_m(0) = (m-1)\theta_m\left(\frac{1}{m-1}\right), \quad (\text{S3a})$$

$$\bar{\theta}''_m(0) = (m-1)(m-2) \left[\theta_m\left(\frac{2}{m-1}\right) - 2\theta_m\left(\frac{1}{m-1}\right) \right]. \quad (\text{S3b})$$

Combining Eqs. (S1), (S2) and (S3), we have self-consistent equations to solve for both the invasion threshold and the tricritical points.

Invasion threshold

We can identify the invasion threshold β_c for a fixed structure given by $\tilde{P}(k)$ and $\hat{P}(m)$, and for a fixed exponent $\nu = \alpha$, assuming $P(\tau) = C_\alpha \tau^{-\alpha-1}$. Combining Eqs. (S1a), (S2) and (S3a), the constraint $G'(0) = 1$ becomes

$$\left(\frac{\langle m(m-1)\theta_m\left(\frac{1}{m-1}\right) \rangle}{\langle m \rangle} \right) \left(\frac{\langle k^2 \rangle}{\langle k \rangle} \right) = \mu. \quad (\text{S4})$$

The left-hand side is intuitively interpreted as the average number of new infections caused by an infected node in a single time step near the absorbing state.

To get more insights, let us use the asymptotic development $\theta_m(1/m-1) \propto \beta^\nu [f(m)]^\nu (m-1)^{-\nu}$, valid when $\beta f(m)/(m-1) \ll 1$ and $\mathcal{T}\beta f(m)/(m-1) \gg 1$. We obtain

$$\beta_c \propto \left(\frac{\mu \langle m \rangle \langle k \rangle}{\langle m(m-1)^{1-\nu} [f(m)]^\nu \rangle \langle k^2 \rangle} \right)^{1/\nu}. \quad (\text{S5})$$

In the case $f(m) = \text{cst.}$, we see that having $\nu < 1$ induces a very small value for the invasion threshold.

Tricritical points

For a fixed structure given by $\tilde{P}(k)$ and $\hat{P}(m)$, the tricritical points (β_c, ν_c) are solutions to both $G'(0) = 1$ and $G''(0) = 0$. We substitute $\bar{\theta}'(0) = \mu/\langle k \rangle$ in (S1b) to obtain

$$G''(0) = \frac{1}{\mu} \left\{ \langle k^2 \rangle \bar{\theta}''(0) - \left(\langle k^2(k-1) \rangle + \frac{2\langle k^3 \rangle}{\mu} \right) \frac{\mu^2}{\langle k \rangle^2} \right\}. \quad (\text{S6})$$

Since the second term is strictly positive, it is necessary that $\bar{\theta}''(0) > 0$ to have a tricritical point.

Using again the asymptotic expansion for $\theta_m(\rho)$ in combination with Eq. (S2) and (S3b), we get

$$\bar{\theta}''(0) \propto \frac{\beta^\nu}{\langle m \rangle} \left\langle m(m-1)^{1-\nu}(m-2)[f(m)]^\nu (2^\nu - 2) \right\rangle. \quad (\text{S7})$$

The tricritical point is evaluated at $\beta = \beta_c$, hence we can substitute the asymptotic expansion for the invasion threshold [Eq. (S5)] to have an expression that only depends on ν ,

$$\bar{\theta}''(0) \propto \mu \frac{\langle k \rangle}{\langle k^2 \rangle} \frac{\left\langle m(m-1)^{1-\nu}(m-2)[f(m)]^\nu (2^\nu - 2) \right\rangle}{\left\langle m(m-1)^{1-\nu} [f(m)]^\nu \right\rangle}. \quad (\text{S8})$$

We get three insights from Eqs. (S6) and (S8).

1. It is necessary that $\nu > 1$ to have a tricritical point, but not sufficient: it depends on the first three moments of $\tilde{P}(k)$, and in a more complicated manner on the distribution $\hat{P}(m)$.
2. It is necessary to have $\hat{P}(m) > 0$ for at least one value $m > 2$, i.e., environments of size $m = 2$ cannot lead to a discontinuous phase transition.
3. A more heterogeneous $\tilde{P}(k)$ will typically require a larger ν to reach a tricritical point. Indeed, if we keep $\langle k \rangle$ fixed, but increase the value for the second and third moments (using a broader distribution for instance), the negative term on the right in Eq. (S6) increases, while the positive term is invariant.

ROBUSTNESS TO OTHER SOURCES OF HETEROGENEITY

The results put forward in this paper highlight the role of the burstiness of interactions for the emergence of nonlinear infection kernels. The heterogeneity of degree k_r and environment sizes m_γ is also incorporated in the modeling approach we use in the main text. In this section, we show that adding other layers of heterogeneity do not alter the form of the kernel $\theta_m(\rho)$ as derived in the main text. We demonstrate it in the case $K = 1$, but the reasoning can be systematically applied for $K > 1$.

Heterogeneity of environment

The attack rate in an environment is certainly affected by the conditions of the environment itself: for instance, non-ventilated places might be more prone to infections than better ventilated ones. Let us assume that β is an i.i.d random variable for each environment, drawn from an arbitrary distribution $Q(\beta)$. Recall that $\tau_c^{-1} \equiv f(m)\beta\rho$.

Without loss of generality, we assume that $Q(\beta)$ is well-behaved. More specifically, we assume that $Q(\beta) = o(\beta^{-n}) \forall n \in \mathbb{N}$ for $\beta \rightarrow \infty$. If $Q(\beta)$ was a power law, it would play a similar role as $P(\tau)$, since β and τ appear side by side in the definition of $T_{\tau,m}$. Also, if τ and β were both distributed as power laws, then the distribution $R(x)$ for $x = \tau\beta$ would be a mixture of power-law distributions [2]. The tail of $R(x)$ would be dominated by the slowest decaying distribution, either $Q(\beta)$ or $P(\tau)$. In all cases, we would perform the same analysis as in the main text.

We further assume that there is a range $\mathcal{B} \equiv [\beta_1, \beta_2]$ with $\int_{\beta_1}^{\beta_2} Q(\beta)d\beta$ sufficiently large, such that for all $\beta \in \mathcal{B}$, $\beta f(m)\rho \ll 1$ and $\mathcal{T} \gg (\beta f(m)\rho)^{-1}$.

For $K = 1$, then $\theta_m(\rho)$ is given by

$$\theta_m(\rho) = \int_1^{\mathcal{T}} \int_0^\infty Q(\beta) \left[1 - e^{-\tau/\tau_c} \right] P(\tau) d\beta d\tau. \quad (\text{S9})$$

Using $P(\tau) = C_\alpha \tau^{-\alpha-1}$ and integrating this by parts, we obtain

$$\begin{aligned} \theta_m(\rho) &= \frac{C_\alpha}{\alpha} \int_0^\infty Q(\beta) \left[1 - e^{-1/\tau_c} - \mathcal{T}^{-\alpha} + \mathcal{T}^{-\alpha} e^{-\mathcal{T}/\tau_c} \right] d\beta \\ &\quad + \frac{C_\alpha}{(\alpha)} \int_0^\infty Q(\beta) \tau_c^{-\alpha} \left\{ \int_{1/\tau_c}^{\mathcal{T}/\tau_c} u^{-\alpha} e^{-u} du \right\} d\beta, \\ &\simeq \frac{C_\alpha}{\alpha} \int_0^\infty Q(\beta) \left[1 - e^{-\beta f(m)\rho} \right] d\beta \\ &\quad + \frac{C_\alpha [f(m)\rho]^\alpha}{\alpha} \int_0^\infty Q(\beta) \beta^\alpha \left\{ \int_{\beta f(m)\rho}^{\beta f(m)\rho \mathcal{T}} u^{-\alpha} e^{-u} du \right\} d\beta. \end{aligned}$$

Since $Q(\beta)$ is well-behaved, the first term is $\mathcal{O}(\rho)$. For the second term, we limit the range of integration on β to \mathcal{B} , and find lower and upper bounds for $\theta_m(\rho)$. Finally, performing an asymptotic expansion for $\beta f(m)\rho \ll 1$ and $\beta f(m)\rho \mathcal{T} \gg 1$ reveals that both the lower and upper bounds have the same behavior,

$$\theta_m(\rho) \propto \begin{cases} \rho^\alpha & \text{if } \alpha \in (0, 1), \\ \rho & \text{if } \alpha \geq 1, \end{cases}$$

Therefore, under previous assumptions, the heterogeneous environment conditions do not change the scaling behavior of $\theta_m(\rho)$. This is validated in Fig. S1.

Heterogeneity of individual infectiousness

Similarly, all infectious individuals are not equivalent. For instance, the viral load within an infectious individual depends on the time since infection. Or more simply, people's behavior varies widely, some follow diligently public health recommendations (hand-washing, social distancing, etc.) and some do not. This motivates assigning an i.i.d. random variable β_j for all infectious individuals $j \in \{1, \dots, i\}$, where $i \equiv \rho(m-1)$, with arbitrary distribution $Q(\beta)$. To treat this case, we need to consider infectious individuals independently, with κ_j the number of occasions for disease transmission with infectious node j . It is also a Poisson random variable, with relation $\kappa = \sum_j \kappa_j$. Equation (1) in the main text becomes

$$T_{\tau,m}(\rho|\{\beta_j\}_{j=1}^i) = 1 - \prod_{j=1}^i \sum_{\kappa_j=0}^{\infty} \pi(\kappa_j) (1 - \beta_j)^{\kappa_j}, \quad (\text{S10})$$

where

$$\pi(\kappa_j) = \frac{\tilde{z}^{\kappa_j} e^{-\kappa_j}}{\kappa_j!},$$

and $\tilde{z} \equiv f(m)\tau/(m-1)$. We can rewrite it as

$$\begin{aligned} T_{\tau,m}(\rho|\{\beta_j\}_{j=1}^i) &= 1 - \prod_{j=1}^i e^{-\tilde{z}\beta_j}, \\ &= 1 - e^{-\tilde{z} \sum_j \beta_j}, \end{aligned} \quad (\text{S11})$$

which has a form very similar to Eq. (1) in the main text. Note that for a threshold $K = 2$, we obtain

$$T_{\tau,m}(\rho|\{\beta_j\}_{j=1}^i) = 1 - \left(1 + \tilde{z} \sum_j \beta_j \right) e^{-\tilde{z} \sum_j \beta_j},$$

which is similar to what we would obtain with Eq. (2) in the main text.

Note that these equations can be rewritten using the mean transmission probability $\tilde{\beta} \equiv \sum_j \beta_j / i$, for which there exists a well-defined distribution $\tilde{Q}(\tilde{\beta})$ (asymptotically normal for $i \gg 1$). We average Eq. (S11) over $\tilde{Q}(\tilde{\beta})$ to obtain

$$T_{\tau,m}(\rho) = 1 - \int_0^1 \tilde{Q}(\tilde{\beta}) e^{-i\tilde{\beta}} d\tilde{\beta}. \quad (\text{S12})$$

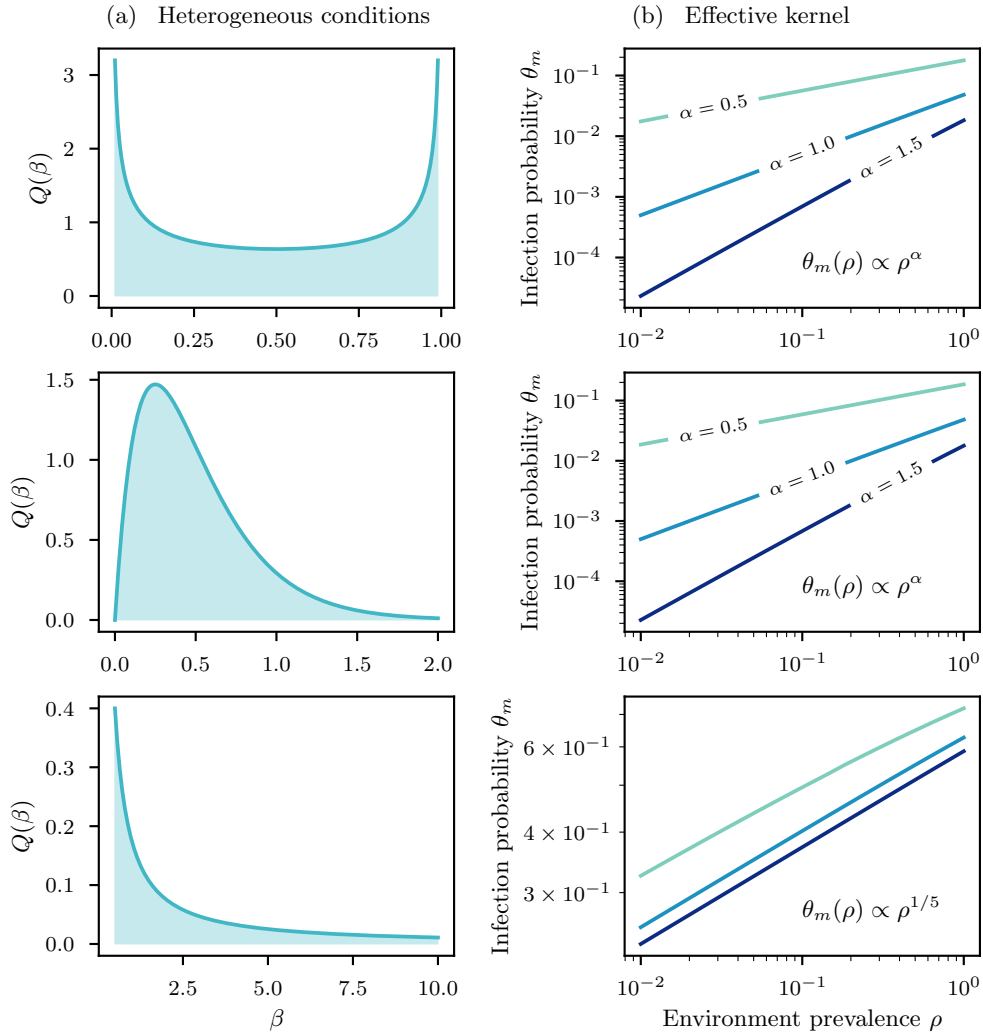


FIG. S1. Nonlinear infection kernels are robust to heterogeneous infectiousness. (a) From top to bottom, we assume β distributed according to $Q(\beta) = \sqrt{\beta(1-\beta)}/\pi$, a beta distribution, $Q(\beta) = 16\beta e^{-4\beta}$, a gamma distribution, and $Q(\beta) \propto \beta^{-6/5}$, a power-law distribution with $\beta \in [0.5, \infty)$. (b) Effective kernel using a threshold ($K = 2$) with power-law distribution of participation time $P(\tau) \propto \tau^{-\alpha-1}$, a time window $\mathcal{T} \rightarrow \infty$ and $f(m) = 0.1$. For $\tau_c^{-1} \ll 1$, the infection probability has power law scaling $\theta_m(\rho) \propto \rho^\nu$ with $\nu = \alpha$ for the well-behaved $Q(\beta)$ —beta and gamma distributions—, and $\nu = 1/5$ for the power-law distribution $Q(\beta)$, since it is more heterogeneous than $P(\tau)$.

Consequently, using $\rho = i/(m-1)$, we find

$$\theta_m(\rho) = \int_1^{\mathcal{T}} \int_0^1 \tilde{Q}(\tilde{\beta}) [1 - e^{-f(m)\tau\rho\tilde{\beta}}] P(\tau) d\tilde{\beta} d\tau.$$

The form of this integral is completely equivalent to Eq. (S9), which means the behavior of $\theta_m(\rho)$ is again unaltered under the same assumptions. In fact, the statistic $\tilde{\beta}$ can be seen as a random variable that again characterizes the infectiousness of the environment.

Binomial distribution for the participation to hyperedges

In the main text, it is assumed that a node r will interact in k_r different environments during a time window \mathcal{T} . More realistically, we can consider that an individual participate to an adjacent hyperedge with probability p , hence the effective degree of a node for a time window is drawn from a binomial distribution with parameters k_r and p .

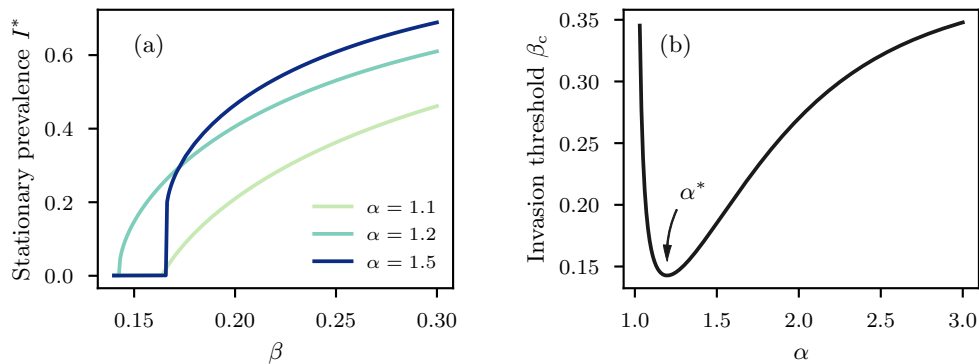


FIG. S2. Impact of a fixed mean participation time $\langle \tau \rangle = 1$. We use a threshold ($K = 2$) with a power-law participation time distribution $P(\tau) \propto \tau^{-\alpha-1}$, $\tau \in [(\alpha - 1)/\alpha, \infty)$, and $f(m) = 1$. We also use Poisson distributions for both $\tilde{P}(k)$ and $\hat{P}(m)$, with $\langle k \rangle = 5$ and $\langle m \rangle = 10$, and set $\mu = 0.05$. (a) Upper branch of the bifurcation diagram, highlighting the differences with a fixed τ_{\min} as in Fig. 2 in the main text. For a sufficiently large β , I^* now grows with α . (b) The invasion threshold β_c is minimized for a value $\alpha^* \approx 1.2$, tends toward infinity in the limit $\alpha \rightarrow 1$, and converges to a certain value in the limit $\alpha \rightarrow \infty$.

This can be incorporated in our approach simply by using

$$P(\tau) = C_\alpha p \tau^{-\alpha-1} + (1 - p) \delta(\tau) .$$

The effect is simply to map $\theta_m(\rho) \mapsto p\theta_m(\rho)$, leaving its scaling with ρ unaltered. Therefore, the whole phenomenology is preserved.

PARTICIPATION TIME DISTRIBUTION WITH A FIXED MEAN

In the main text, we fixed the minimal participation time to $\tau_{\min} = 1$, but we let $\langle \tau \rangle$ vary with α . Here we show the consequence of fixing $\langle \tau \rangle = 1$, and to let τ_{\min} vary. For the sake of simplicity, we assume $\mathcal{T} \rightarrow \infty$. For a power-law distribution $P(\tau) = C_\alpha \tau^{-\alpha-1}$, this is achieved if we set $\tau_{\min} = (\alpha - 1)/\alpha$. Note that it is only possible for $\alpha > 1$, i.e., when the mean is well-defined.

As shown in Fig. S2, keeping a fixed $\langle \tau \rangle$ reveals another story for the bifurcation diagram. For a sufficiently large β , we now have that I^* grows with α —a homogeneous participation time lead to bigger outbreaks—, which is the opposite of what we found for a fixed τ_{\min} . Moreover, the invasion threshold is now a non-monotonic function of α . It is minimized for some value $\alpha^* \approx 1.2$, and the early spread of an epidemic would be maximized for this α^* .

QUENCHED MEAN-FIELD MODEL

Instead of the annealed description presented in the text, one could consider a *quenched* structure, more appropriate to represent the recurrent participation to the same environment by an individual—one usually goes to the same grocery stores, office, etc.

We can define a SIS model on a hypergraph, similar in form to Ref. [3] with N nodes $r = 1, 2, \dots, N$ and M hyperedges $\gamma = 1, 2, \dots, M$. We define $t = 1, 2, \dots$ as the subsequent time slices, and $\rho_r(t)$ the marginal probability that a node r is infected. Under a quenched mean-field assumption—ignoring dynamical correlations—, the dynamics can be written as

$$\rho_r(t+1) = (1 - \mu)\rho_r(t) + (1 - \rho_r(t))\Psi_r . \quad (\text{S13})$$

Here μ indicates the probability of recovery and Ψ_r indicates the probability that individual r is infected as a consequence of its exposure to at least one of its environments (hyperedges),

$$\Psi_r = 1 - \prod_{\gamma \in \mathcal{N}(r)} [(1 - \bar{\theta}_{r,\gamma})] , \quad (\text{S14})$$

with $\bar{\theta}_{r,\gamma}$ indicating the average probability that node r is infected in environment γ . Interestingly we note that Ψ_r can also be

expressed in terms of the adjacency matrix of the hypergraph as

$$\Psi_r = 1 - \exp \left[\sum_{\gamma} A_{r\gamma} \log (1 - \bar{\theta}_{r,\gamma}) \right]. \quad (\text{S15})$$

To close the system of equations, we express $\bar{\theta}_{r,\gamma}$ as an average over a Poisson binomial distribution,

$$\bar{\theta}_{r,\gamma} = \sum_{A \in F_{r,\gamma}(i)} \prod_{s \in A} \rho_s \prod_{u \in A^c} (1 - \rho_u) \theta_m \left(\frac{i}{m_{\gamma} - 1} \right), \quad (\text{S16})$$

where $F_{r,\gamma}(i)$ is the set of all subsets of nodes A participating to environment γ , except node r , and such that $|A| = i$. We note A^c the complement of A , i.e., the set of all nodes participating to the environment, except node r and those in A .

-
- [1] M. Karsai, H.-H. Jo, and K. Kaski, *Bursty Human Dynamics* (Springer International Publishing, 2018).
 [2] S. Nadarajah, Exact distribution of the product of m gamma and n Pareto random variables, *J. Comput. Appl. Math.* **235**, 4496 (2011).
 [3] G. Ferraz de Arruda, G. Petri, and Y. Moreno, Social contagion models on hypergraphs, *Phys. Rev. Research* **2**, 023032 (2020).